# Model for General Acid−Base Catalysis by the Hammerhead Ribozyme: pH−Activity Relationships of G8 and G12 Variants at the Putative Active Site†

Joonhee Han and John M. Burke*

*Department of Microbiology and Molecular Genetics, University of Vermont, 95 Carrigan Drive, 220 Stafford Hall, Burlington, Vermont 05405*

*Received September 22, 2004; Revised Manuscript Received March 17, 2005*

ABSTRACT: We have used nucleobase substitution and kinetic analysis to test the hypothesis that hammerhead catalysis occurs by a general acid−base mechanism, in which nucleobases are directly involved in deprotonation of the attacking 2′-hydroxyl group and protonation of the 5′-oxygen that serves as the leaving group in the cleavage reaction. We demonstrate that simultaneous substitution of two important nucleobases, G8 and G12, with 2,6-diaminopurine shifts the pH optimum of the cleavage reaction from greater than 9.5 to approximately 6.8 in two different hammerhead constructs. Controls involving substitution with other nucleobases and combinations of nucleobases at G5, G8, and/or G12 do not show this behavior. The observed changes in the pH−rate behavior are consistent with a mechanism in which N1 protonation−deprotonation events of guanine or 2,6-diaminopurine at positions 8 and 12 are essential for catalysis. Further support for the participation of G8 and G12 comes from photochemical cross-linking experiments, which show that G8 and G12 can stack upon the two substrate nucleobases at the reactive linkage, G(or U)1.1 and C17 (Heckman, J. E., Lambert, D., and Burke, J. M. (2005) Photocrosslinking detects a compact active structure of the hammerhead ribozyme, *Biochemistry 44,* 4148−4156). Together, these results support a model in which the hammerhead undergoes a transient conformational change into a catalytically active structure, in which stacking of G8 and G12 upon the nucleobases spanning the cleavage site provides an appropriate architecture for general acid−base catalysis. The hammerhead and hairpin ribozymes may share similarities in the organization of their active sites and their catalytic mechanism.

The hammerhead ribozyme is a small RNA endonuclease, found in a wide range of organisms, that is known to be essential for RNA processing reactions required for the propagation of virus-related RNA replicons in plant cells, including the satellite RNA associated with tobacco ringspot virus (*2, 3*). First described in 1986 (*4, 5*), the hammerhead has been intensively studied by numerous investigators using a full complement of biochemical, biophysical, and combinatorial methods (*6*−*16*). The reaction catalyzed by the hammerhead ribozyme (Figure 1) is a reversible RNA cleavage reaction that occurs with formation of products containing 2′,3′-cyclic phosphate and 5′-hydroxyl termini (*2, 3*). In this regard, it is similar to the reaction catalyzed by the hairpin, hepatitis delta and VS ribozymes, and some protein ribonucleases (*17, 18*).

Although early mechanistic studies focused on the possible role of inner-sphere catalysis by metal ions, there is strong evidence that metal ions are not required for the reaction (*19*−*21*). Rather, cations are required to fold the ribozyme into its active tertiary structure, but the reaction can proceed without the formation of direct contacts between RNA and metal ions. Therefore, the hammerhead RNA contains all of the functional groups that are required for catalytic function.

The solution structure of the hammerhead ribozyme has been studied by NMR, FRET, hydroxyl radical protection, and transient electric birefringence methods (*8, 15, 22*−*24*), and they show that a Y-shaped ribozyme−substrate complex is the dominant conformation in solution. This structure appears to be quite similar to the published crystallographic structures (*11, 14*), with relatively small differences likely attributable to differences in crystallographic packing and/or the constructs chosen. A notable characteristic of these structures is the lack of extensive interaction between the two domains which constitute the "catalytic core", each containing several functionally important nucleotides (*16*).

There is general agreement that the crystallographic and solution structures represent an inactive ground state, and that a transient conformational change within the ribozyme−substrate complex is required to attain the active structure. However, there are differences of opinion as to whether this conformational change is a local rearrangement of the substrate cleavage site (*25, 26*), or a larger-scale event that includes the formation of contacts between the two domains that are not reflected in the crystal structure (*27, 28*). These issues are reviewed in detail by Blount and Uhlenbeck (*29*).

Recently, larger hammerhead constructs have been studied that include additional native sequences that stabilize an interaction between nucleotides distal to helices 1 and 2, lower the concentration of cations required for optimal activity, and promote ligation (*30, 31*). This interaction acts

† This work is supported by Grant GM65552 to J.M.B. from the National Institutes of Health.

* To whom correspondence should be addressed. Tel: (802) 656-8503. Fax: (802) 656-8749. E-mail: John.Burke@uvm.edu.

10.1021/bi047941z CCC: $30.25 
Published on Web 05/05/2005

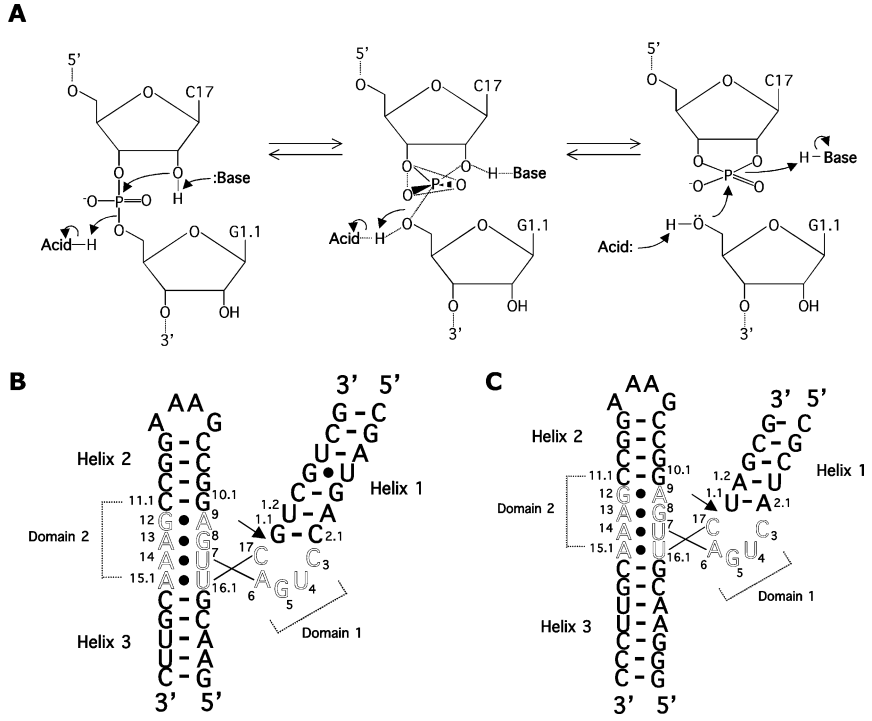


FIGURE 1: (A) The hammerhead ribozyme catalyzes sequence-specific phosphodiester bond cleavage, generating 2′,3′-cyclic phosphate and 5′-hydroxyl termini. The cleavage reaction is initiated by deprotonation of the 2′-OH and proceeds by an in-line attack mechanism. The sequences and secondary structures of hammerhead ribozymes 16 (B) and 16.4 (C). The outlined nucleotides represent the conserved sequences believed to constitute the catalytic core. This ribozyme cleaves the phosphodiester bond between C17 and N1.1, and the arrow indicates the cleavage site. The numbering is according to Hertel (*48*).

to reduce the concentration of cations required to fold into the ground state structure (*10*), but there is as yet no evidence that they influence the transition from the ground state to the active structure.

Bevilacqua has analyzed published data to show that the pH−rate relationships of hairpin ribozymes are consistent with a general acid−base mechanism involving two nucleobases of the ribozyme, one with a high p$K_A$ (G or U), and one with a low p$K_A$ (A or C) (*32*). This model accounts for the observed rate vs pH curve that displays an extensive, flat plateau from pH 5 to 9. There is substantial biochemical and crystallographic evidence that N1 of G8 (p$K_A$ 9.6) is the titratable group with the high p$K_A$ (*33*−*35*). Notably, replacement of G8 with 2-aminopurine (p$K_A$ 3.8) or 2,6-diaminopurine (p$K_A$ 5.1) results in a characteristic bell-shaped rate vs pH curve with very low activity at higher pH (*33*). N1 of A38 is likely to be the titratable group with the lower p$K_A$ (*32*).

In contrast, the hammerhead cleavage reaction shows a characteristic log-linear increase of reaction rate with pH (*36*). The plot of rate vs pH shows little leveling off at the highest pH values studied, which are limited by alkaline hydrolysis of ribozyme and substrate. Previously, this behavior was rationalized by a model in which a metal ion−hydroxide complex was required for catalysis (*17, 36*). However, the finding that inner-sphere coordination by metals is not required for hammerhead catalysis makes this model less attractive (*19*−*21*).

Here, we propose that the hammerhead's rate vs pH behavior can be explained by general acid−base chemistry, in which both of the functional groups involved in catalysis have a high p$K_A$. We present evidence that these catalytic groups are the N1s of two conserved nucleobases within the catalytic core, G8 and G12. In separate work, G8 and G12 have been shown to crosslink to the substrate nucleotides at the scissile linkage and a G8−C17 crosslink retains catalytic activity (*1*). Together, this work supports a model in which hammerhead reactions are catalyzed by an acid−base mechanism following a transient conformational change in which G8 and G12 come to occupy catalytic positions within the active site.

## MATERIALS AND METHODS

*Materials.* All oligonucleotides were generated by solid-phase synthesis using nucleotide phosphoramidites purchased from Glen Research or ChemGenes and then deprotected and purified by denaturing polyacrylamide gel electrophoresis and HPLC, as described previously (*37, 38*).

*Methods. Ribozyme Cleavage Assays.* Catalytic activities of the hammerhead ribozyme and its variants were measured under single-turnover conditions. Ribozymes (1−3 $\mu$M) and 5′-$^{32}$P-end-labeled substrate (<5 nM) in 50 mM reaction buffer were heat-denatured at 95 °C for 2 min and preincubated at 25 °C for 10 min for equilibration and folding. The cleavage reactions were initiated by adding $MgCl_2$ solution (final concentration 25 mM) and carried out at 25 °C in 50 mM Mes (pH 5.5 to 6.5), 50 mM Mops (pH 6.75 to 7.0), 50 mM Hepes[1] (pH 7.25 to 8.0), and 50 mM Tris (pH 8.5 and 9.0). One-microliter aliquots were withdrawn at each time point and quenched with 10 volumes of 95% formamide

[1] Abbreviations: Hepes, 2-[4-(2-hydroxyethyl)-1-piperazinyl]ethanesulfonic acid; Mops, 3-(*N*-morpholino)propanesulfonic acid; Mes, 2-morpholinoethanesulfonic acid, monohydrate; Tris, tris(hydroxymethyl)aminomethane; I, inosine; 2AP, 2-aminopurine; diAP, 2,6-diaminopurine.

loading solution. The cleavage reactions were analyzed by 20% polyacrylamide 8 M urea gel electrophoresis and quantified using a Bio-Rad Molecular Imager FX system. The cleavage rates were calculated by curve-fitting using Microcal Origin software as described (*22*, *33*).

*Hydroxyl Radical Footprinting Assays.* The hydroxyl radical footprinting assays were carried out as described previously with modifications (*22*, *39*). The total volumes of the reactions were 10 $\mu$L. In order for the ribozyme−substrate complex to fold, ribozymes (0.5 $\mu$M) and 5′-$^{32}$P-end-labeled noncleavable substrate (<5 nM) including a 2′-deoxy substitution at position C17 were incubated in 25 mM Hepes, pH 7.0 at 25 °C for 10 min in the presence or absence of 25 mM $MgCl_2$. Next, 0.8 $\mu$L of Fe(II)-EDTA solution (12.5 mM EDTA, 10 mM $Fe(NH_4)_2(SO_4)_2$), 0.8 $\mu$L of $H_2O_2$ (0.375% v/v), and 0.8 $\mu$L of sodium ascorbate (60 mM) were added sequentially onto the inside wall of the reaction tube. The hydroxyl radical cleavage reactions were initiated by quick centrifugation of the above reaction tubes. The reactions were quenched by adding 2 $\mu$L of tRNA (10 mg/mL) and 10 $\mu$L of 3 M sodium acetate diluted in 88 $\mu$L of $H_2O$, followed by ethanol precipitation. The cleaved products were analyzed by 20% polyacrylamide 8 M urea gel electrophoresis and quantified using a Bio-Rad Molecular Imager FX system.

## RESULTS AND DISCUSSION

The catalytic core of the hammerhead (Figure 1) is composed of two domains, consisting of 5 (domain 1) and 8 (domain 2) nucleotides, which form a number of intradomain, noncanonical interactions in the crystallographic structures (*11*, *14*). A number of these nucleotides (C3, G5, A6, G8, A9, G12, A13, A14) are critical for cleavage activity (*40*, *41*), but only guanosine and uridine have the high p$K_A$ values required by the model for general acid−base catalysis described above. Since there are no essential uridines within the catalytic core, we focused our attention on the three critical guanosines, G5, G8, and G12. Deoxyribose G5 substitutions have previously been shown to interfere with folding into the native tertiary structure (*22*, *42*, *43*), but these results cannot rule out a further role for the nucleobase in catalysis.

Hammerhead 16 (*44*) ribozyme variants containing nucleobase substitutions were generated by solid-phase synthesis. The three essential guanosines (N1 p$K_A$ 9.6) were individually replaced with inosine (I, N1 p$K_A$ 8.7), 2,6-diaminopurine (diAP, N1 p$K_A$ 5.1), and 2-aminopurine (2AP, N1 p$K_A$ 3.8), and ribozyme activity was examined as a function of pH (Figure 2). Cleavage rates were measured under single-turnover conditions (1 $\mu$M ribozyme and <5 nM substrate) in the presence of 25 mM $MgCl_2$ and 50 mM reaction buffer over a pH range of 5.5 to 9.0.

Substitutions of G5 showed significant inhibition at all pH values tested (Figure 2B). The activities of the 2AP5 and I5 variants were diminished by 3 orders of magnitude relative to the unmodified ribozyme, while the activity of the diAP variant was diminished by 4 orders of magnitude. Because all four of the rate vs pH plots paralleled one another, we conclude that, relative to the unmodified ribozyme, the extent of inhibition of the G5 variants was independent of pH.

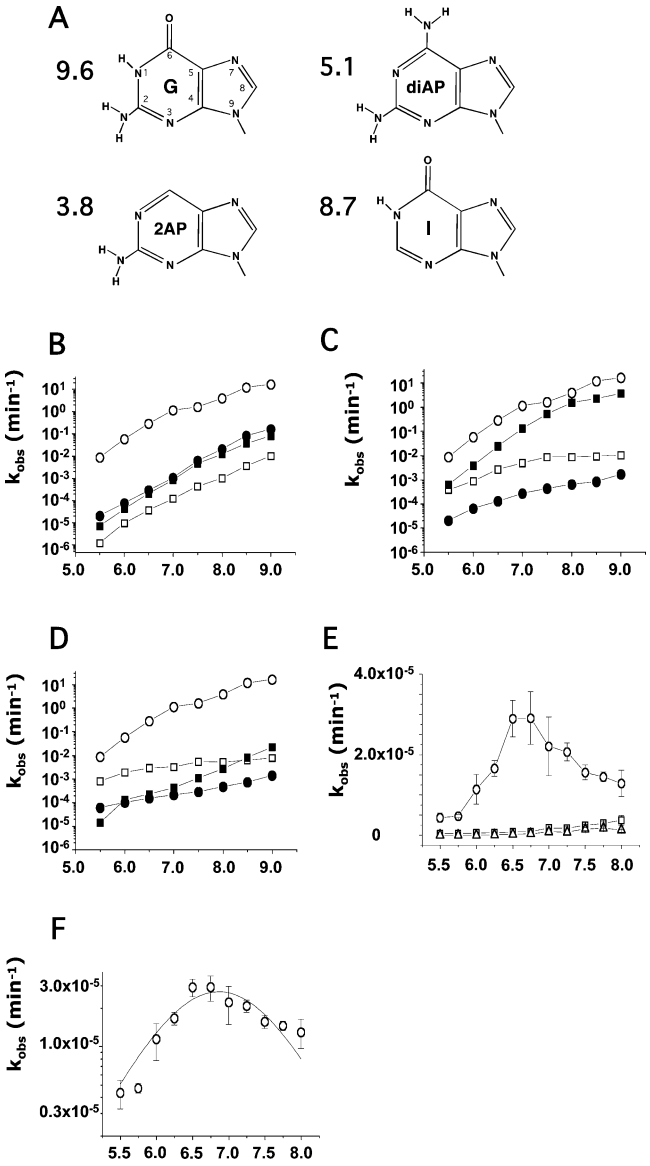


FIGURE 2: (A) Structure and N1 p$K_A$ of guanine (G) and guanine analogues, 2,6-diaminopurine (diAP), 2-aminopurine (2AP), inosine (I). (B, C, and D) Cleavage rate−pH profile of hammerhead 16 ribozyme variants with guanosine (○), 2,6-diaminopurine (□), 2-aminopurine (●) or inosine (■). (B) G variants at position 5. (C) G variants at position 8. (D) G variants at position 12. The cleavage reactions were carried out at 25 °C in 25 mM $MgCl_2$ and 50 mM Mes (pH 5.5−6.5), 50 mM Mops (pH 7.0), 50 mM Hepes (pH 7.5 and 8.0), and 50 mM Tris (pH 8.5 and 9.0) under single-turnover conditions. (E) Cleavage rate−pH profile of hammerhead 16 ribozyme variants with diAP8:diAP12 (○), diAP5:diAP12 (□), and diAP5:diAP8 (△). (F) The rate−pH profile of hammerhead 16 diAP8:diAP12 ribozyme was fitted to the equation $k_{obs} = k_{max}/(1 + 10^{pH-pK_A} + 10^{pK_A'-pH})$ (*49*). The cleavage rate−pH profiles of the doubly substituted variants (E and F) represent the average of three sets of experiments. Other profiles (B, C, and D) are from a single experiment, but are consistent with those obtained under a variety of ionic concentrations, using different ribozyme constructs and concentrations (see, for example, Figure 3).

Substitutions of G8 and G12 showed an important difference: the extent of inhibition showed strong variation as a function of pH when G8 or G12 was substituted with 2AP or with diAP, but not when substituted with inosine (Figure 2C,D). In the case of position 8, inosine reduced cleavage rate by approximately 1 order of magnitude over the full pH range that was examined (Figure 2C). I12 reduced the

cleavage rate to a greater extent than I8 (3 orders of magnitude), but like I8, the extent of inhibition was independent of pH. For diAP8, the inhibition varied strongly as a function of pH, with a reduction of cleavage rate by 1 order of magnitude at pH 5.5, but more than 3 orders of magnitude at pH 9.0. The same general observation also holds true for diAP12, 2AP8, and 2AP12, where the extent of inhibition increases with pH from 5.5 to 9.0.

Referring to the Bevilacqua formulation of acid−base catalysis for the hairpin ribozyme (*32*), these results are consistent with a model in which hammerhead bases G8 and G12, but not G5, function in protonation−deprotonation events at the active site. It is noteworthy that the pH−rate profiles of the hammerheads with single 2AP or diAP substitutions at positions 8 or 12 are rather similar to that of the unmodified hairpin ribozyme (*33, 45*). In each case, our interpretation is that one of the two nucleobases at the putative active site has a high p$K_A$, while the other has a low p$K_A$.

To further test this hypothesis, we synthesized hammerheads containing all pairwise combinations of diAP at positions 5, 8, and 12, and examined their activities as a function of pH (Figure 2E,F). Two of the combinations, diAP5:diAP8 and diAP5:diAP12, showed essentially no cleavage over the full range of pH values tested. In sharp contrast, the diAP8:diAP12 combination yielded a roughly bell-shaped rate vs cleavage curve, with an increase in rate from pH 5.5 to 6.5 and a decrease from pH 6.75 to 8.0.

These results are consistent with a model in which G8 and G12 function in acid−base reactions at the active site. However, other interpretations may be possible. For example, this behavior could be idiosyncratic to the hammerhead 16 construct that was used for the above work. Alternatively, the substitutions could induce pH-dependent misfolding of the ribozyme−substrate complex.

To ensure that the modified activity vs pH behavior was not an artifact of the hammerhead 16 construct, we examined the effects of the diAP substitutions in a different context, hammerhead 16.4 (Figure 1C), which cleaves its substrate at a rate approximately 10-fold greater than hammerhead 16 (*46*) (Figure 3). Single diAP substitutions at positions 5, 8, and 12 and the double substitution diAP8:diAP12 affected the rate vs pH relationship in the same manner as for hammerhead 16 (Figure 3A). Indeed, the activity plateau reached by the single substitutions at positions 8 and 12 is more clearly defined than were the results for hammerhead 16. These results suggest that the differences in the pH optima of the singly and doubly substituted ribozymes may be a common feature of kinetically well-behaved hammerheads.

Results for hammerhead 16.4 doubly substituted with diAP at positions 8 and 12 are shown in Figure 3B. Results were best fitted by a theoretical curve representing general acid−base catalysis by two functional groups with p$K_A$ values of 6.87 and 6.91, using the model described by Bevilacqua (*32*).

To examine the possibility of misfolding induced by base substitution, we conducted hydroxyl radical protection experiments on hammerhead 16 and its variants. This method is useful in monitoring folding of the ribozyme−substrate complex into its ground state tertiary structure, which is similar to the crystallographic structure. Hydroxyl radical protection has the advantage of being able to monitor

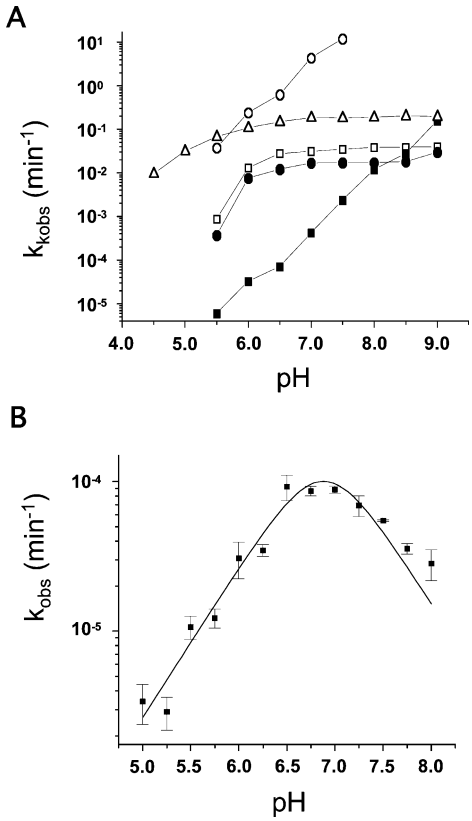


FIGURE 3: (A) Cleavage rate−pH profile of hammerhead 16.4 ribozyme variants. Unmodified ribozyme (○), 2,6-diaminopurine at position 12 (□), 2,6-diaminopurine at position 8 (●), or 2,6-diaminopurine at position 5 (■). The cleavage reactions were carried out at 25 °C in 25 mM $MgCl_2$ and 50 mM Mes (pH 5.5−6.5), 50 mM Mops (pH 7.0), 50 mM Hepes (pH 7.5 and 8.0), and 50 mM Tris (pH 8.5 and 9.0) under single-turnover conditions. The cleavage rate−pH profile of the hairpin ribozyme (△) was taken from Pinard et al. (*33*) and superimposed into this figure. (B) Cleavage activity of hammerhead 16.4 diAP8:diAP12 ribozyme at various pH values. The cleavage reactions were carried out at 25 °C in 25 mM $MgCl_2$ and 50 mM sodium acetate (pH 5.0), 50 mM Mes (pH 5.25−6.5), 50 mM Mops (pH 6.75 and 7.0), and 50 mM Hepes (pH 7.25−8.0) for 2 days under single-turnover conditions. The data of hammerhead 16.4 diAP8:diAP12 ribozyme were fitted as described in the caption to Figure 2. The cleavage rate−pH profiles of single diAP substitutions at position 5, 8, or 12 (A) represent a single set of experiments; the cleavage rate−pH profile of the doubly substituted variant (B) represents the average of two sets of experiments.

multiple sites within the complex at single nucleotide resolution (*47*). The disadvantage is that, like crystallography and FRET, it does not necessarily provide information about the active structure, if different from the ground state. We conducted hydroxyl radical protection experiments using the hammerhead 16 variants described above, and focused on the backbone protection pattern at four sites within the catalytic core: the two nucleotides in domain 1 that constitute the cleavage site (C17 and G1.1), and two protected nucleotides within domain 2 (U7 and G8) (Figure 4). A 2′-deoxy G5 variant was used as a negative control (*42, 43*). The extent of protection was diminished in several cases. In general, substitutions of G5 and G8 with other purines resulted in less protection at all sites, while substitutions of G12 had very little effect on the extent of protection. In all cases, examination of the overall protection patterns showed no changes in the identity of the protected nucleotides. We

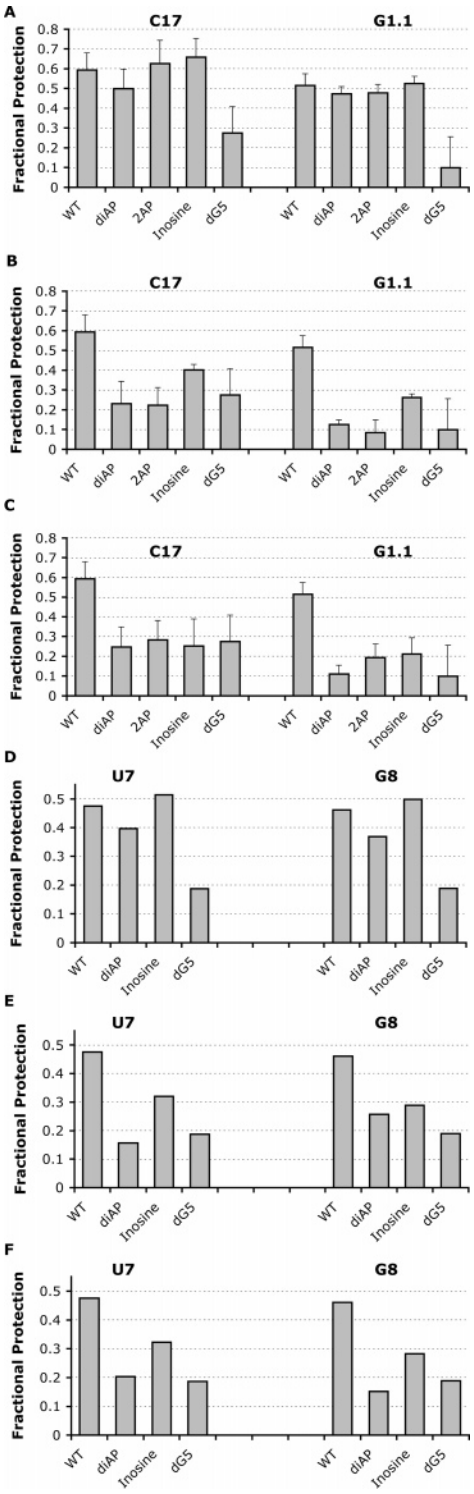


FIGURE 4: Hydroxyl radical footprinting assays of hammerhead 16 ribozyme variants. Backbone protections of the cleavage site (C17 and G1.1) and domain 2 (U7 and G8) were measured. The reactions were carried out at 25 °C in 25 mM $MgCl_2$ and 25 mM Hepes (pH 7.0) with indicated hammerhead 16 ribozyme variants. (A) Fractional protection of G12 variants at C17 and G1.1. (B) Fractional protection of G8 variants at C17 and G1.1. (C) Fractional protection of G5 variants at C17 and G1.1. (D) Fractional protection of G12 variants at U7 and G8. (E) Fractional protection of G8 variants at U7 and G8. (F) Fractional protection of G5 variants at U7 and G8. The fractional protections of G5, G8, and G12 variants at C17 and G1.1 (A, B, and C) were obtained from at least three replicate experiments. The fractional protections of G5, G8, and G12 variants at U7 and G8 (D, E, and F) were obtained from a single set of experiments.

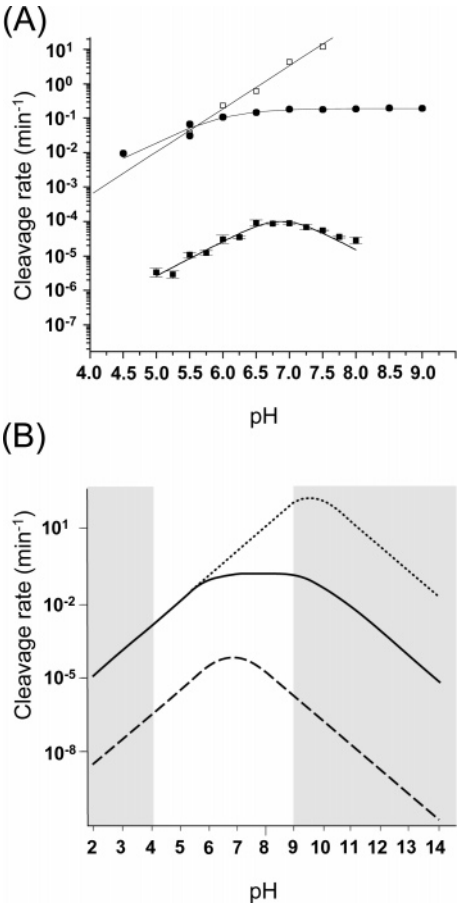


FIGURE 5: (A) pH−rate profiles of hammerhead 16.4 and variants at positions 8 and 12. Results (data points) are shown for the unmodified hammerhead 16.4 ribozyme (□), hammerhead 16.4 diAP8:diAP12 double variant (■), and the hairpin ribozyme (●). Hairpin ribozyme data are taken from ref *33*. Lines represent curve fits of the experimental data obtained as described in the caption to Figure 2. (B) Simulation of the pH−rate profiles of the same three ribozymes from pH 2 to 14. In these simulations we assumed the following values for p$K_A$ and p$K_A'$. Unmodified hammerhead 16.4, 9.6 and 9.6 (values for free guanine). Hammerhead 16.4 diAP8:diAP12 double variant, 6.91 and 6.87 (obtained from fitting experimental results from Figure 3B). Hairpin ribozyme, 5.94 and 9.6 (*32*, *33*). Gray regions show the pH ranges where experimental data cannot be obtained. Simulations used the equation described in the caption to Figure 2.

conclude that G12 substitutions have little effect on ground state tertiary folding, while G8 and G5 substitutions partially inhibit folding to the ground state, but do not induce detectable misfolding events. Importantly, the very large extents of inhibition of the substituted ribozymes (multiple orders of magnitude) do not correlate with differences in ground state tertiary folding.

Our experimental results are well-described by a simple model for general acid−base catalysis in which the N1 functional groups of purine nucleobases at positions 8 and 12 catalyze the essential protonation events at the reaction sites in the hammerhead cleavage and ligation reactions. G5 variants strongly inhibit cleavage, but do so in a pH-independent manner that is consistent with a role in folding to the active structure. Figure 5A shows a comparison of the rate−pH profiles of the wild-type hammerhead ribozyme (log-linear increase with pH), the hairpin ribozyme (increase followed by long plateau), and the double-diAP hammerhead 16.4 substituted at 8 and 12 (roughly bell-shaped). Figure

5B shows a set of rate−pH simulations, demonstrating the profiles that would be expected from acid−base catalysis by three ribozymes, each with two catalytic groups: one in which both groups have high N1 p$K_A$s; one with a mix of one low and one high p$K_A$; and one with two fairly low p$K_A$s (derived from the experimental values above). The unshaded area shows the pH range in which RNA cleavage reactions can be conducted. It can be seen that the data curves of the three ribozymes in Figure 5A correlate well with the portions of the simulation curves obtained between pH 4 and pH 9 (Figure 5B).

Although our results are fully consistent with acid−base catalysis by G8 and G12, we cannot completely rule out other hypothetical models, for example a pH-dependent conformational change driven by G8 and G12, in which other unidentified moieties are responsible for catalysis.

In separate work, we have shown that G8 and G12 can be covalently crosslinked to the bases spanning the substrate cleavage site (*1*), providing evidence for a transient conformational change in which the cleavage site nucleobases C17 and G1.1 move from their positions in the ground state tertiary structure to positions stacked on G8 and G12. This orientation may be similar to that observed in the tertiary structure of the hairpin ribozyme, where catalytic bases G8 and A38 stack on cleavage site bases A−1 and G+1 (*33*, *34*).

## ACKNOWLEDGMENT

We would like to thank Dr. Joyce Heckman and Dr. Ken Hampel for comments and support, Dr. Christina Pecore for assistance in data analysis, and Anne MacLeod for assistance in manuscript preparation.

## REFERENCES

1. Heckman, J. E., Lambert, D., and Burke, J. M. (2005) Photocrosslinking detects a compact active structure of the hammerhead ribozyme, *Biochemistry 44*, 4148−4156.
2. Forster, A. C., and Symons, R. H. (1987) Self-cleavage of virusoid RNA is performed by the proposed 55-nucleotide active site, *Cell 50*, 9−16.
3. Uhlenbeck, O. C. (1987) A small catalytic oligoribonucleotide, *Nature 328*, 596−600.
4. Hutchins, C. J., Rathjen, P. D., Forster, A. C., and Symons, R. H. (1986) Self-cleavage of plus and minus RNA transcripts of avocado sunblotch viroid, *Nucleic Acids Res. 14*, 3627−3640.
5. Prody, G. A., Bakos, J. T., Buzayan, J. M., Schneider, I. R., and Breuning, G. (1986) Autolytic processing of dimeric plant virus satellite RNA, *Science 321*, 1577−1580.
6. Bondensgaard, K., Mollova, E. T., and Pardi, A. (2002) The global conformation of the hammerhead ribozyme determined using residual dipolar couplings, *Biochemistry 41*, 11532−11542.
7. Derrick, W. B., Greef, C. H., Caruthers, M. H., and Uhlenbeck, O. C. (2000) Hammerhead cleavage of the phosphorodithioate linkage, *Biochemistry 39*, 4947−4954.
8. Gast, F. U., Amiri, K. M., and Hagerman, P. J. (1994) Interhelix geometry of stems I and II of a self-cleaving hammerhead RNA, *Biochemistry 33*, 1788−1796.
9. Hermann, T., Auffinger, P., and Westhof, E. (1998) Molecular dynamics investigations of hammerhead ribozyme RNA, *Eur. Biophys. J. 27*, 153−165.
10. Penedo, J. C., Wilson, T. J., Jayasena, S. D., Khvorova, A., and Lilley, D. M. (2004) Folding of the natural hammerhead ribozyme is enhanced by interaction of auxiliary elements, *RNA 10*, 880−888.
11. Pley, H. W., Flaherty, K. M., and McKay, D. B. (1994) Three-dimensional structure of a hammerhead ribozyme, *Nature 372*, 68−74.
12. Rueda, D., Wick, K., McDowell, S. E., and Walter, N. G. (2003) Diffusely bound $Mg^{2+}$ ions slightly reorient stems I and II of the hammerhead ribozyme to increase the probability of formation of the catalytic core, *Biochemistry 42*, 9924−9936.
13. Salehi-Ashtiani, K., and Szostak, J. W. (2001) In vitro evolution suggests multiple origins for the hammerhead ribozyme, *Nature 414*, 82−84.
14. Scott, W. G., Finch, J. T., and Klug, A. (1995) The crystal structure of an all-RNA hammerhead ribozyme: a proposed mechanism for RNA catalytic cleavage, *Cell 81*, 991−1002.
15. Tuschl, T., Gohlke, C., Jovin, T. M., Westhof, E., and Eckstein, F. (1994) A three-dimensional model for the hammerhead ribozyme based on fluorescence measurements, *Science 266*, 785−789.
16. Wedekind, J. E., and McKay, D. B. (1998) Crystallographic structures of the hammerhead ribozyme: relationship to ribozyme folding and catalysis, *Annu. Rev. Biophys. Biomol. Struct. 27*, 475−502.
17. Takagi, Y., Warashina, M., Stec, W. J., Yoshinari, K., and Taira, K. (2001) Recent advances in the elucidation of the mechanisms of action of ribozymes, *Nucleic Acids Res. 29*, 1815−1834.
18. Roberts, G. C., Dennis, E. A., Meadows, D. H., Cohen, J. S., and Jardetzky, O. (1969) The mechanism of action of ribonuclease, *Proc. Natl. Acad. Sci. U.S.A. 62*, 1151−1158.
19. Murray, J. B., Seyhan, A. A., Walter, N. G., Burke, J. M., and Scott, W. G. (1998) The hammerhead, hairpin and VS ribozymes are catalytically proficient in monovalent cations alone, *Chem. Biol. 5*, 587−595.
20. Curtis, E. A., and Bartel, D. P. (2001) The hammerhead cleavage reaction in monovalent cations, *RNA 7*, 546−552.
21. O'Rear, J. L., Wang, S., Feig, A. L., Beigelman, L., Uhlenbeck, O. C., and Herschlag, D. (2001) Comparison of the hammerhead cleavage reactions stimulated by monovalent and divalent cations, *RNA 7*, 537−545.
22. Hampel, K. J., and Burke, J. M. (2003) Solvent protection of the hammerhead ribozyme in the ground state: evidence for a cation-assisted conformational change leading to catalysis, *Biochemistry 42*, 4421−4429.
23. Bassi, G. S., Mollegaard, N. E., Murchie, A. I., von Kitzing, E., and Lilley, D. M. (1995) Ionic interactions and the global conformations of the hammerhead ribozyme, *Nat. Struct. Biol. 2*, 45−55.
24. Maderia, M., Hunsicker, L. M., and DeRose, V. J. (2000) Metal-phosphate interactions in the hammerhead ribozyme observed by 31P NMR and phosphorothioate substitutions, *Biochemistry 39*, 12113−12120.
25. Scott, W. G. (2001) Ribozyme catalysis via orbital steering, *J. Mol. Biol. 311*, 989−999.
26. Murray, J. B., Dunham, C. M., and Scott, W. G. (2002) A pH-dependent conformational change, rather than the chemical step, appears to be rate-limiting in the hammerhead ribozyme cleavage reaction, *J. Mol. Biol. 315*, 121−130.
27. Wang, S., Karbstein, K., Peracchi, A., Beigelman, L., and Herschlag, D. (1999) Identification of the hammerhead ribozyme metal ion binding site responsible for rescue of the deleterious effect of a cleavage site phosphorothioate, *Biochemistry 38*, 14363−14378.
28. Blount, K. F., Grover, N. L., Mokler, V., Beigelman, L., and Uhlenbeck, O. C. (2002) Steric interference modification of the hammerhead ribozyme, *Chem. Biol. 9*, 1009−1016.
29. Blount, K. F., and Uhlenbeck, O. C. (2005) The Structure-Function Dilemma of the Hammerhead Ribozyme, *Annu. Rev. Biophys. Biomol. Struct.*, in press.
30. Canny, M. D., Jucker, F. M., Kellogg, E., Khvorova, A., Jayasena, S. D., and Pardi, A. (2004) Fast cleavage kinetics of a natural hammerhead ribozyme, *J. Am. Chem. Soc. 126*, 10848−10849.
31. Khvorova, A., Lescoute, A., Westhof, E., and Jayasena, S. D. (2003) Sequence elements outside the hammerhead ribozyme catalytic core enable intracellular activity, *Nat. Struct. Biol. 10*, 708−712.
32. Bevilacqua, P. C. (2003) Mechanistic considerations for general acid-base catalysis by RNA: revisiting the mechanism of the hairpin ribozyme, *Biochemistry 42*, 2259−2265.
33. Pinard, R., Hampel, K. J., Heckman, J. E., Lambert, D., Chan, P. A., Major, F., and Burke, J. M. (2001) Functional involvement of G8 in the hairpin ribozyme cleavage mechanism, *EMBO J. 20*, 6434−6442.

34. Rupert, P. B., and Ferre-D'Amare, A. R. (2001) Crystal structure of a hairpin ribozyme-inhibitor complex with implications for catalysis, *Nature 410*, 780−786.
35. Rupert, P. B., Massey, A. P., Sigurdsson, S. T., and Ferre-D'Amare, A. R. (2002) Transition state stabilization by a catalytic RNA, *Science 298*, 1421−1424.
36. Dahm, S. C., Derrick, W. B., and Uhlenbeck, O. C. (1993) Evidence for the role of solvated metal hydroxide in the hammerhead cleavage mechanism, *Biochemistry 32*, 13040−13045.
37. Walter, N. G., Yang, N., and Burke, J. M. (2000) Probing non-selective cation binding in the hairpin ribozyme with Tb(III), *J. Mol. Biol. 298*, 539−555.
38. Butcher, S. E., and Burke, J. M. (1994) A photo-cross-linkable tertiary structure motif found in functionally distinct RNA molecules is essential for catalytic function of the hairpin ribozyme, *Biochemistry 33*, 992−999.
39. Hampel, K. J., Walter, N. G., and Burke, J. M. (1998) The solvent-protected core of the hairpin ribozyme-substrate complex, *Biochemistry 37*, 14672−14682.
40. McKay, D. B. (1996) Structure and function of the hammerhead ribozyme: an unfinished story, *RNA 2*, 395−403.
41. Ruffner, D. E., Stormo, G. D., and Uhlenbeck, O. C. (1990) Sequence requirements of the hammerhead RNA self-cleavage reaction, *Biochemistry 29*, 10695−10702.
42. Bassi, G. S., Murchie, A. I., and Lilley, D. M. (1996) The ion-induced folding of the hammerhead ribozyme: core sequence changes that perturb folding into the active conformation, *RNA 2*, 756−768.
43. Bassi, G. S., Mollegaard, N. E., Murchie, A. I., and Lilley, D. M. (1999) RNA folding and misfolding of the hammerhead ribozyme, *Biochemistry 38*, 3345−3354.
44. Hertel, K. J., Herschlag, D., and Uhlenbeck, O. C. (1994) A kinetic and thermodynamic framework for the hammerhead ribozyme reaction, *Biochemistry 33*, 3374−3385.
45. Nesbitt, S., Hegg, L. A., and Fedor, M. J. (1997) An unusual pH-independent and metal-ion-independent mechanism for hairpin ribozyme catalysis, *Chem. Biol. 4*, 619−630.
46. Clouet-d'Orval, B., and Uhlenbeck, O. C. (1997) Hammerhead ribozymes with a faster cleavage rate, *Biochemistry 36*, 9087−9092.
47. Celander, D. W., and Cech, T. R. (1991) Visualizing the higher order folding of a catalytic RNA molecule, *Science 251*, 401−407.
48. Hertel, K. J., Pardi, A., Uhlenbeck, O. C., Koizumi, M., Ohtsuka, E., Uesugi, S., Cedergren, R., Eckstein, F., Gerlach, W. L., Hodgson, R., et al. (1992) Numbering system for the hammerhead, *Nucleic Acids Res. 20*, 3252.
49. Lebruska, L. L., Kuzmine, I. I., and Fedor, M. J. (2002) Rescue of an abasic hairpin ribozyme by cationic nucleobases. Evidence for a novel mechanism of RNA catalysis, *Chem. Biol. 9*, 465−473.

BI047941Z